

Effect of a potential softness on the solid-liquid transition in a two-dimensional core-softened potential system

D.E. Dudalov,¹ Yu.D. Fomin,^{1,2} E.N. Tsiok,¹ and V.N. Ryzhov^{1,2}

¹ *Institute for High Pressure Physics RAS, 142190 Kaluzhskoe shosse, 14, Troitsk, Moscow, Russia*

² *Moscow Institute of Physics and Technology, 141700 Moscow, Russia*

(Dated: October 5, 2018)

In the present paper, using a molecular dynamics simulation, we study a nature of melting of a two-dimensional (2D) system of classical particles interacting through a purely repulsive isotropic core-softened potential which is used for the qualitative description of the anomalous behavior of water and some other liquids. We show that the melting scenario drastically depends on the potential softness and changes with increasing the width of the smooth repulsive shoulder. While at small width of the repulsive shoulder the melting transition exhibits what appears to be weakly first-order behavior, at larger values of the width a reentrant-melting transition occurs upon compression for not too high pressures, and in the low density part of the 2D phase diagram melting is a continuous two-stage transition, with an intermediate hexatic phase in accordance with the Kosterlitz-Thouless-Halperin-Nelson-Young (KTHNY) scenario. On the other hand, at high density part of the phase diagram one first-order transition takes place. These results may be useful for the qualitative understanding the behavior of water confined between two hydrophobic plates.

PACS numbers: 61.20.Gy, 61.20.Ne, 64.60.Kw

INTRODUCTION

Water plays an important role in many natural processes where it is confined or at contact with substrates. Examples can be found in different fields of geology, biology, chemical engineering because water can be confined in rocks, in biological cells, at contact with surfaces of proteins, in biological membranes, etc [1–4]. In three dimensions the qualitative behavior of water, including the waterlike anomalies, can be described using the core-softened potentials with two length scales [5–25]). The liquids with these potentials demonstrate anomalous behavior in some regions of thermodynamic parameters: their phase diagrams have regions where a thermal expansion coefficient is negative (density anomaly), self-diffusivity increases upon compression (diffusion anomaly), and the structural order of the system decreases with increasing pressure (structural anomaly). This kind of behavior is characteristic of a number of real fluids, the most common and well known example is water. Later on it was discovered that many other substances also demonstrate similar behavior. Some typical examples are silica, silicon, phosphorus, etc. A lot of different core-softened potentials were introduced (see, for example, reviews [11, 12]). However, it should be noted that in general the existence of two length scales is not compulsory to induce the occurrence of the anomalies. For example, for the models studied in Ref. [18, 19] it was shown that the existence of two distinct repulsive length scales is not a necessary condition for the occurrence of anomalous phase behavior.

In general, the observation, that confined fluids microscopically relax and flow with different characteristic time scales than bulk liquids is hardly surprising. Confining

boundaries bias the spatial distribution of the constituent molecules and the ways by which those molecules can dynamically rearrange. These effects play important roles in the thermodynamics of the confined systems and influence the topology of the phase diagram. The general motivation for the study of different confined fluids follows from the observation that there are many real physical and biological phenomena and processes that depend on the properties of such systems and play an important role in the different fields of modern technology such as fabrication of nanomaterials, nanotribology, adhesion, and nanotechnology [26, 27].

It is well known that the nature of spatial ordering of a molecular system depends on the dimensionality of the space to which it is confined. As it was shown by Mermin [28], in 2D the long-range crystalline order is destroyed by the thermal fluctuations and has the quasi-long-range character. However, the real long range order does exist in this case - this is the order in orientations of bonds between the particle and its nearest neighbor (bond-orientational order).

During the several decades, the controversy about the nature of the 2D melting transition is lasting. Now it is widely accepted the theory by Halperin, Nelson, and Young [29–31], based on the Kosterlitz-Thouless ideas [32] (KTHNY theory). In accordance with this theory, the scenario of two-dimensional melting is fundamentally different from the melting of three-dimensional systems. In 2D case the transition between a crystal and an isotropic liquid can occur by means of two continuous transitions which correspond to dissociation of bound dislocation and disclination pairs, respectively. Dissociation of the dislocation pairs at some temperature T_m destroys the quasi-long-range translational order. The resulting

phase has the short-range translational order, but the quasi-long-range bond orientational order. This phase is called the hexatic phase. The isotropic liquid appears as a result of dissociation of the disclination pairs at some temperature T_i .

The KTHNY theory have got an experimental support from the experiments with electrons on helium [33] and the colloidal model system with repulsive magnetic dipole-dipole interaction [34–38]. In the case of colloidal suspension, confined in a channel, reducing the channel size changes the system behavior from three-dimensional to two-dimensional, and colloidal monolayer displays continuous $2D$ melting [40–43].

At the same time, a conventional first-order transition between a two-dimensional solid and an isotropic liquid can also occur ([44–51]). For example, as it was shown in [50, 51], at low disclination core energy system can melt through one first-order transition as a result of the dissociation of the disclination quadrupoles.

Despite numerous experimental and simulation studies, the situation is controversial - KTHNY theory seems universal and independent on the pair potential of the system, however, the systems with very short range or hard core potentials demonstrates the coexisting phases (weak first-order transition), while the melting scenarios for the soft repulsive particles favor the KTHNY theory [18, 27, 52–74].

Even for simplest potential systems, including hard and soft disks or Lennard-Jones potentials, despite the tendency to the weak first-order melting transition, the simulation results are conflicting [52–65]. The "toy" model for the investigation of the melting transition in $2D$, hard-disk system, have been studied in a large number of computer simulations without unambiguous conclusion about the melting scenario [53–56, 61]. It was even suggested an unexpected possibility of the first-order hexatic-isotropic liquid transition [59, 60].

In general, one can conclude that the melting transition strongly depends on the pair interaction in the system. For instance, as shown by Bladon and Frenkel [67] in the framework of the computer simulations, a $2D$ solid of particles with short-range attraction can be unstable to dislocation unbinding in a region that is clearly thermodynamically stable with respect to the isotropic fluid. The system supports an isostructural solid-solid transition. In the vicinity of the critical temperature for this isostructural transition, fluctuations can induce formation of a hexatic phase. As the range of attraction part of the potential grows, the hexatic phase region becomes larger and moves toward the melting line.

In Refs. [48, 49] the density functional calculations have shown that the $2D$ square-well system can demonstrate both first-order and continuous melting phase transitions depending on the width of the attractive well.

Recently, Prestipino et al [69] presented a Monte Carlo simulation study of the phase behavior of two-

dimensional classical particles repelling each other through an isotropic Gaussian potential [75–79]. They have shown, that as in the analogous three-dimensional case, a reentrant-melting transition occurs along with a spectrum of waterlike anomalies in the fluid phase. However, in $2D$ melting is a continuous two-stage transition, with a narrow intermediate hexatic phase, in agreement with the KTHNY scenario.

In Ref. [18], Prestipino, Saija, Giaquinta considered the behavior of the system with the extremely soft Yoshida and Kamakura potential [80]. It was shown that in the model there exist three different crystal phases, one of them with square symmetry and the other two triangular. The most interesting fact is that the triangular solids melt into a hexatic fluid, while the square solid is directly transformed on heating into an isotropic fluid through a first-order transition. A whole spectrum of waterlike anomalies also exists for this model potential.

In our recent papers [72–74] we presented a computer simulation study of the phase diagram and anomalous behavior of two-dimensional core-softened potential system [5–10] with the soft core $\sigma_1 = 1.35$ (see Eq. (1)). As in Ref. [18], we found three different crystal phases, one of them with square symmetry and the other two triangular. In the low density part of the $2D$ phase diagram, melting of the triangular phase is a continuous two-stage transition, with an intermediate hexatic phase. All available evidences support the KTHNY scenario for this melting transition. At high density part of the phase diagram square and triangular phases melt through one first-order transition.

On the other hand, in [22] the phase diagram was studied for a square-shoulder square-well potential in two dimensions that has been previously shown to exhibit liquid anomalies consistent with a metastable liquid-liquid critical point [20]. It was shown that all the melting lines are first order, despite a small range of metastability.

This paper extends our previous results to the set of systems which are characterized by the different softness, in order to study the influence of the softness on the melting scenarios. We present a simulation study of phase behavior of the core-softened system, introduced in our previous publications [5–10, 72–74], in two dimensions. The main goal is to compare the phase diagrams of the systems with the potentials of the increasing softness and to reveal the influence of the softness of the potential on the melting scenarios.

The paper is organized as follows: Sec. II presents the system and methods, Sec. III describes the results and their discussion, and finally Sec. IV contains conclusions.

SYSTEMS AND METHODS

The system we study in the present simulations is the smooth repulsive shoulder system (SRSS) introduced in

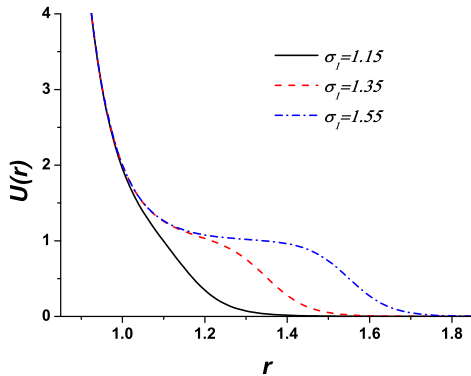


FIG. 1: The potential (1) with three different soft-core diameters: $\sigma_1 = 1.15; 1.35; 1.55$.

our previous publications [5–10, 72–74]:

$$U(r) = \varepsilon \left(\frac{\sigma}{r} \right)^n + \frac{1}{2} \varepsilon (1 - \tanh(k_1 \{r - \sigma_1\})). \quad (1)$$

where $n = 14$ and $k_1 \sigma = 10.0$. σ is the hard-core diameter. We simulate the systems with three different soft-core diameters: $\sigma_1/\sigma = 1.15; 1.35; 1.55$. (see Fig. 1).

In the remainder of this paper we use the dimensionless quantities, which in $2D$ have the form: $\tilde{\mathbf{r}} \equiv \mathbf{r}/\sigma$, $\tilde{P} \equiv P\sigma^2/\varepsilon$, $\tilde{V} \equiv V/N\sigma^2 \equiv 1/\tilde{\rho}$, $\tilde{T} \equiv k_B T/\varepsilon$, $\tilde{\sigma}_1 = \sigma_1/\sigma$. Since we will use only these reduced variables, the tildes will be omitted.

As it was discussed before [5], the system with this potential corresponds to the quasibinary mixture of spheres with the diameters σ and σ_1 .

As it was shown in [5–10], in $3D$ system of particles interacting through a core-softened potential (1) exhibits a number of unusual features, including reentrant melting, a maximum on the melting curve, superfragile glass behavior, and thermodynamic and dynamic anomalies similar to the ones found in water and silica.

In our previous publications [48, 49] it was shown that one has to distinguish two temperatures which characterize the melting transition in two dimensions. The mean-field temperature T_{MF} corresponds to the disappearance of the modulus of the Fourier transform of the local density $\rho_{\mathbf{G}}$ and another one, T_m , is the temperature at which the singular fluctuations of the phase of the order parameter (free dislocations) appear in the system. In the case $T_m < T_{MF}$ one can expect that the system melts through the continuous Kosterlitz-Thouless transition, T_{MF} being the limit of the metastable solid phase. If $T_m > T_{MF}$, the system melts via a first-order transition. T_{MF} can be obtained from the double-tangent construction for the free energies of liquid and solid phases, but in order to determine T_m and T_i and conclude whether the melting occurs through the KTHNY scenario, the additional analysis is necessary.

In order to distinguish between the first-order and continuous melting, we also used the criteria described in Ref. [61]. We calculated the pressure P versus density ρ along the isotherms, the bond orientational ψ_n , $n = 4, 6$ and translational ψ_T order parameters (OPs), which characterize the overall translational and orientational order, and the bond orientational correlation function $G_n(r)$, $n = 4, 6$. In the case of the first-order phase transition the isotherms demonstrate the Van der Waals loops, and OP ψ_n has almost linear behavior in the supposed two-phase region as a function of density. According to the KTHNY scenario [29–31, 61], melting in $2D$ can occur via two continuous transitions (at densities ρ_l and ρ_s) with corresponding pressures P_l and $P_s > P_l$, rather than via a single first-order transition at coexistence pressure P_T (where a fluid of density ρ_l and a solid of density ρ_s will coexist). In this case the isotherms are smooth in contrast with the Van der Waals loops for a first order transition [61].

We use the molecular dynamics simulations of the system in NVT and NVE ensembles (LAMMPS package [83]) with the number of particles between 3200 and 102400. To determine T_{MF} as a function of density, we calculate the Helmholtz free energy for liquid and solid phases and construct a common tangent to them. Because the potential (1) is purely repulsive, there is no liquid-gas transition in the system. In this case, the Helmholtz free energy of the liquid can be calculated by integrating the equation of state along an isotherm [82]:

$$\frac{F(\rho) - F_{id}(\rho)}{Nk_B T} = \frac{1}{k_B T} \int_0^\rho \frac{P(\rho') - \rho' k_B T}{\rho'^2} d\rho'. \quad (2)$$

Free energies of solid phases were calculated in the framework of the method of coupling to the Einstein crystal [82]. Double tangent construction gives the lines of the first order melting transition.

In order to proceed in analysis of the melting scenarios, let us define the translational order parameter ψ_T (TOP), the orientational order parameter Ψ_n (OOP), and the bond-orientational correlation function $G_n(r)$ (OCF) in the conventional way [18, 29, 30, 39, 53, 61, 65, 69].

TOP is taken in the form

$$\psi_T = \frac{1}{N} \left\langle \left| \sum_i e^{i\mathbf{G}\mathbf{r}_i} \right| \right\rangle, \quad (3)$$

where \mathbf{r}_i is the position vector of particle i and \mathbf{G} is the first shell reciprocal-lattice vector of the crystal. It should be noted that ψ_T is nonzero if a solid is oriented consistently with the length and direction of \mathbf{G} . In the simulation, ψ_T is measured on heating of the large enough crystal where the original crystal orientation is mainly preserved. Melting of the crystal phase into hexatic phase or isotropic liquid is determined by the sharp decrease of ψ_T .

To study the orientational order and the hexatic phase, let us define the local order parameter, which measures the n -fold orientational ordering, in the following way:

$$\Psi_n(\mathbf{r}_i) = \frac{1}{n(i)} \sum_{j=1}^{n(i)} e^{in\theta_{ij}}, \quad (4)$$

where θ_{ij} is the angle of the bond between particles i and j with respect to a reference axis and the sum over j is over all $n(i)$ nearest-neighbors of i , found from the Voronoi construction. The global OOP is obtained as an average over all particles:

$$\psi_n = \frac{1}{N} \left\langle \left| \sum_i \Psi_n(\mathbf{r}_i) \right| \right\rangle. \quad (5)$$

It should be noted that $n = 6$ corresponds to the triangular solid and $n = 4$ - to square solid. In a perfect triangular solid $n(i) = 6$, $\theta_{ij} = \pi/3$ and $\psi_6 = 1$.

The bond-orientational correlation function $G_n(r)$ (OCF) is given by the equation:

$$G_n(r) = \langle \Psi_n(\mathbf{r}) \Psi_n^*(\mathbf{0}) \rangle, \quad (6)$$

where $\Psi_n(\mathbf{r})$ is the local bond-orientational order parameter (4).

Both in the isotropic fluid phase and in the hexatic phase, $\psi_n \rightarrow 0$ as $L \rightarrow 0$, where L is the linear size of the system, but the behaviors of $G_n(r)$ are different. The KTHNY theory predicts an algebraic large-distance decay of the OCF in the hexatic phase, which should be contrasted with the exponential asymptotic vanishing of angular correlations in a normal isotropic fluid:

$$G_n(r) = e^{-r/\xi}, r \rightarrow \infty, \rho < \rho_l, \quad (7)$$

$$G_n(r) = r^{-\eta(T)}, r \rightarrow \infty, \rho_l < \rho < \rho_s. \quad (8)$$

Here ξ is the correlation length of the bond orientational order, which diverges as ρ_l is approached. Another prediction of the theory is $\eta = 1/4$ at the hexatic-to-normal isotropic fluid transition point [29–31].

RESULTS AND DISCUSSIONS

In Fig. 2 we plot the phase diagrams of 2D system with the potential (1) for $\sigma_1 = 1.15, 1.35, 1.55$ in $\rho - T$ coordinates, obtained from the double tangent construction calculations. As it was mentioned above, these phase diagrams correspond to the thermodynamic limits of the stability of solid phases and give the first order melting lines. In order to check the possibility of the continuous melting, the further analysis is necessary. One can see that for $\sigma_1 = 1.15$ (Fig. 2(a)) there are only liquid and triangular solid phases, and the phase diagram is similar to the ordinary soft spheres case where the weak first order transition can be expected [39, 62–64].

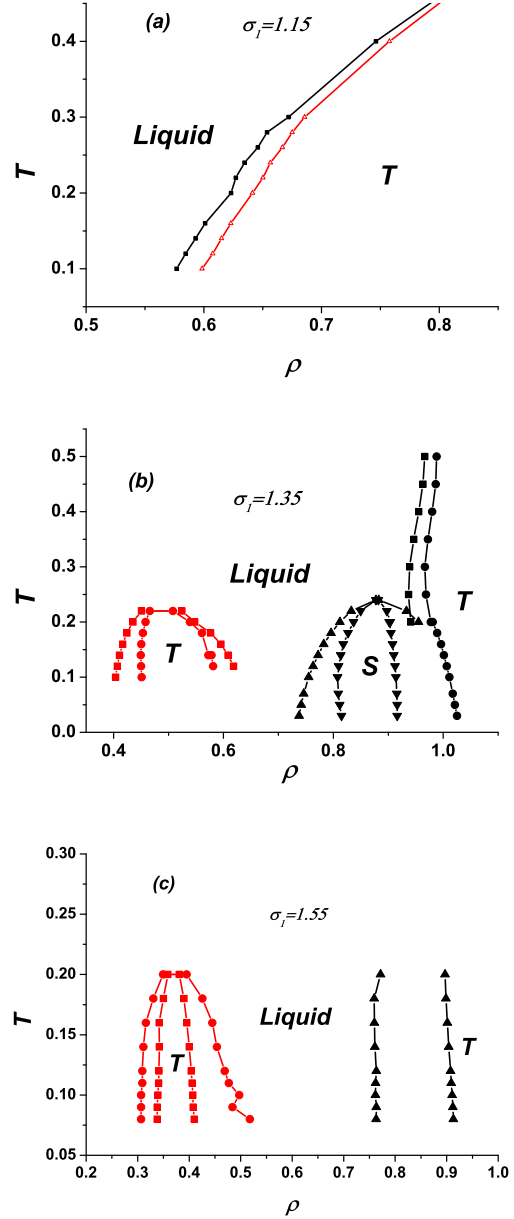


FIG. 2: (Color online) (a) Phase diagram of the 2D system with the potential (1) for $\sigma_1 = 1.15$ in $\rho - T$ plane, where liquid and Triangular (T) phases are shown. (b) Phase diagram for $\sigma_1 = 1.35$, where Triangular (T) and Square (S) phases are shown. (c) Phase diagram of the same system in the $\rho - T$ plane for $\sigma_1 = 1.55$, where liquid and Triangular (T) phases are shown.

For $\sigma_1 = 1.35$ (Fig. 2(b)) the phase diagram is more complex. It was discussed recently [72–74] in detail, and here we recall some main points. There is a clear maximum in the melting curve at low densities. The phase diagram consists of two triangular crystal domains (T) corresponding to close packing of the small and large disks separated by a structural phase transition and square lat-

tice (S). It is important to note that there is a region of the phase diagram where we have not found any stable crystal phase at the temperatures accessible in our simulations. The results of 3D simulations [5, 9] suggest that a glass transition can occur in this region. It should be noted, that for this system the phase diagrams in 2D and 3D are qualitatively similar [5, 74]. They consist in two structures which are close packed in corresponding dimensions: FCC in 3D and triangular in 2D, between which there are some other phases which depend on the parameters of the potential and dimensionality. These structures correspond to the crystalline phases of small spheres (at high densities) and large spheres (at low densities). The qualitative shape of the phase diagrams is determined by the existence of two scales in the potential [5].

The case $\sigma_1 = 1.55$ (see Fig. 2(c)) is qualitatively similar to the previous phase diagram, however, the only triangular solid was found. The "gap" between two ordered parts of the phase diagram is wider, but it seems that in the temperature range explored in our simulations no other simple crystal structure can exist. For instance, we found that the square lattice, which can be supposed to exist in analogy with the case $\sigma_1 = 1.35$ (Fig. 2(b)) is unstable at the temperatures used in our simulations. It should be noted, that in 3D the similar situation takes place [5–10], however, for $\sigma_1 = 1.35$ it was shown [84], that at $T = 0$ there are rather complex crystal structures in the density range, where the "gap" in the phase diagram exists. Unfortunately, we could not find similar structures in 2D.

In Fig. 3 we present the isotherms for $\sigma_1 = 1.15, 1.35, 1.55$ at different temperatures. In Fig. 3(a) there are only Van der Waals loops, corresponding to the first-order liquid-triangular lattice transition. The cases $\sigma_1 = 1.35, 1.55$ are much more complex. Fig. 3(b) represents the low-temperature and high-temperature sets of isotherms for $\sigma_1 = 1.35$. One can see that at low temperatures there are four regions on the isotherms corresponding to the phase transitions, the low density ones being smooth as in the case of liquid-hexatic-solid transition [61] and the high densities part containing the Van der Waals loops characteristic of the first order phase transition. At high temperatures (see Fig. 3(c)) there is only one liquid-triangular lattice first-order transition. From Fig. 3(b) one can guess that the melting of the low-density and high-density parts of the phase diagram occurs with different scenarios: at low densities the KTHNY scenario is probable, while the high density phase melts through the first-order phase transition. As we are going to show in the following, the intermediate region between the low density triangular solid and the (normal) fluid can be qualified as hexatic phase. The case $\sigma_1 = 1.55$ (Fig. 3(c)) is similar to the previous one: the low density part is smooth as in the case of liquid-hexatic-solid transition [61] and the high densities part

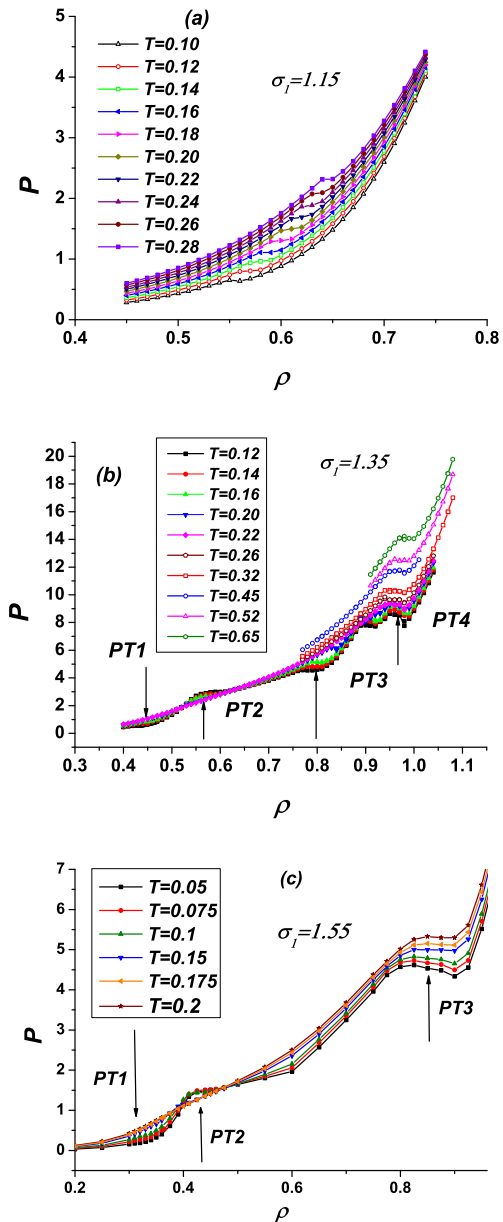


FIG. 3: (Color online) (a) The set of isotherms for $\sigma_1 = 1.15$. (b) The set of isotherms for $\sigma_1 = 1.35$. The arrows mark the phase transitions (compare with Fig. 2(b)). There are the obvious Van der Waals loops at high densities and smooth transitions at low densities. (c) The set of isotherms for $\sigma_1 = 1.55$. The arrows mark the phase transitions (compare with Fig. 2(c)).

demonstrates the Van der Waals loops. It is possible to expect the continuous transition at low densities and the first order transition at high densities.

In Fig. 4, the orientational order parameter (OOP) is presented as a function of density for a set of temperatures for three values of the width of the repulsive shoulder $\sigma_1 = 1.15; 1.35; 1.55$. For $\sigma_1 = 1.15$ (Fig. 4(a)) there

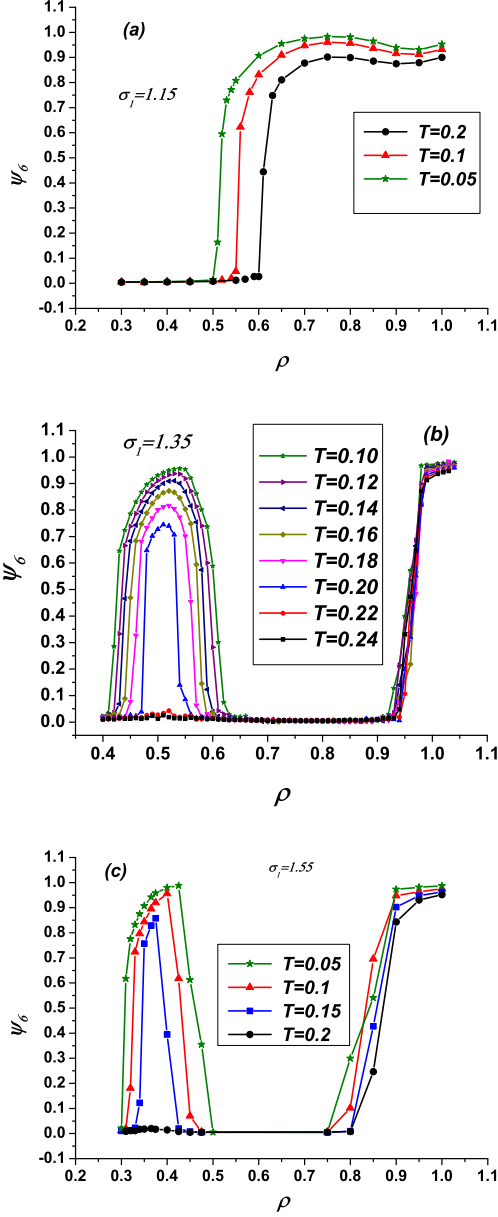


FIG. 4: (Color online) Orientational order parameter ψ_6 as a function of density for different temperatures (a) $\sigma_1 = 1.15$; (b) $\sigma_1 = 1.35$; (c) $\sigma_1 = 1.55$.

is an abrupt quasilinear change of OOP. We attribute this behavior to the weak first-order liquid-triangular solid transition.

As it was mentioned above, the phase diagram for $\sigma_1 = 1.35$ is much more complex. One can see (Fig. 4(b)), the behavior of OOP is different depending on the location on the phase diagram: at the low density part of the phase diagram OOP behaves smoothly while at high densities one can see that the OOP increase almost linearly in the density. Fig. 4(b) also suggests that the melting at low

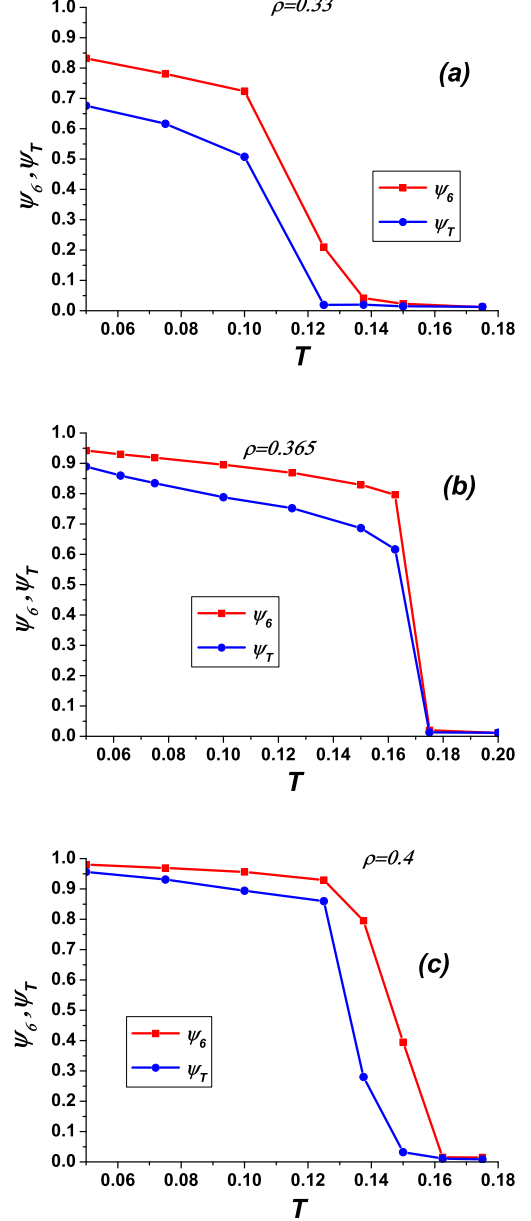


FIG. 5: (Color online) OPs ψ_T and ψ_6 as functions of temperature for $\rho = 0.33$ (a); $\rho = 0.365$ (b); $\rho = 0.4$ (c) in the case of $\sigma_1 = 1.55$. It is the narrow hexatic phase in the cases (a) and (c), while it may be absent for the case (b) (see discussion in the text).

densities is continuous, while at high densities melting transition is of the first order. The similar behavior was found for the case $\sigma_1 = 1.55$.

In Fig. 5, we plot the translational and orientational OPs for $\sigma_1 = 1.55$ and $\rho = 0.33, 0.365, 0.4$ as a function of temperature (an analogous behavior was observed for all the other densities). We see that ψ_T vanishes at a slightly smaller temperature than ψ_6 , which implies that

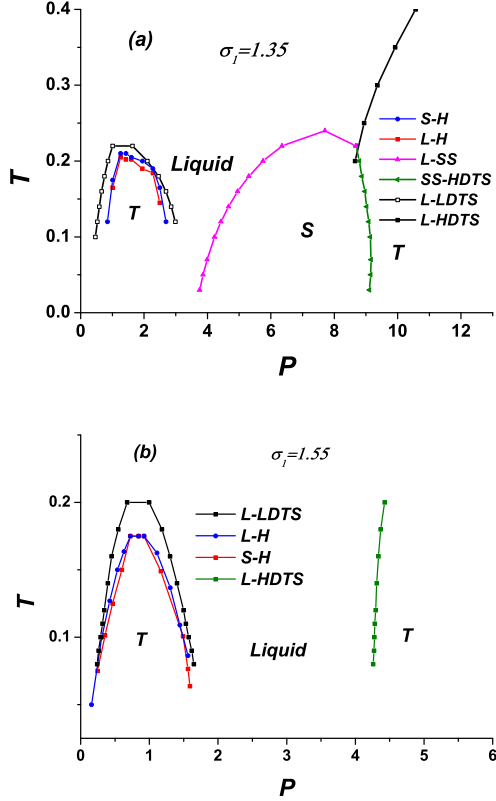


FIG. 6: (Color online) The phase diagrams of the systems with $\sigma_1 = 1.35$ (a) and $\sigma_1 = 1.55$ (b) in $P - T$ plane (compare Fig. 2). There is a narrow hexatic phase region in the low-density part of the phase diagram. The lines of solid-hexatic and hexatic-liquid transitions were obtained with the help of the calculations of ψ_6 and ψ_T (see Fig. 5). S-H means "solid-hexatic", L-H - "liquid-hexatic", L-SS - "liquid-square lattice solid", SS-HDTS - "square lattice solid - high density triangular lattice solid", L-LDTS - "liquid - low density triangular lattice solid", L-HDTS - "liquid - high density triangular lattice solid".

the hexatic phase is confined to a narrow T interval. It is necessary to note, that in the case of the conventional first-order phase transition, the density change at the melting line maximum is equal to zero. For the density close to the maximum on the low density part of the phase diagram ($\rho = 0.48$), the region of the hexatic phase is very narrow, however, we cannot conclusively determine whether the width of the hexatic phase in the maximum point is equal to zero. In the case of $\sigma_1 = 1.35$ the similar behavior takes place [72–74].

In Fig. 6, the phase transition lines of the solid-hexatic and hexatic-liquid transitions, obtained from the calculations of ψ_6 and ψ_T (see, for example, Fig. 5), are shown in comparison with the solid-liquid transition lines (see Fig. 2) in $P - T$ planes for $\sigma_1 = 1.35$ and $\sigma_1 = 1.55$. One can see that the transitions are mainly inside the solid region, obtained in the framework of the free-energy calcu-

lations. This fact also supports the idea that the melting in this region occurs through two continuous transitions.

As it was mentioned above (see discussion after Fig. 2(c)), one can expect that there are some crystal phases inside the "gap" in the phase diagram (Fig. 6(b)), which we could not find. In principle, these phases can be obtained, for example, by the methods used in [84]. From Fig. 3(b) one can suppose that these intermediate phases can exist at low enough temperatures. It should be noted that the symmetry of these possible phases is weaker than the triangular symmetry and favors the first-order melting transition, because, as it was proposed in [18] for the square lattice, in this case the degree of the orientational order is lower than in the triangular crystal.

The errors in calculation of the OOP ψ_6 are less than 1%, while the errors of the translational order parameter ψ_T do not exceed 5%.

A more direct evidence of the hexatic phase emerges from the large-distance behavior of OCF. Fig. 7 shows these functions for three values of the repulsive shoulder widths $\sigma_1 = 1.15; 1.35; 1.55$ across the melting transition at selected densities and temperatures. Calculations of the orientational correlation function are made for 20000-102400 particles. From Fig. 7(a) one can see that the behavior of $G_6(r)$ abruptly changes from isotropic liquid-like with the exponential decay at large distances to the solid-like, where OOF tends to the constant for large r , in accordance with the first-order transition scenario.

In Fig. 7(b) we plot OOF at various densities across the hexatic phase for $\sigma_1 = 1.35$ and $T = 0.12$. Upon increasing ρ from 0.41 to 0.45 there is a qualitative change in the large-distance behavior of $G_6(r)$, from constant (solid) to power-law decay (hexatic fluid), up to exponential decay (normal fluid). Note that, consistently with the KTHNY theory, the decay exponent η is less than $1/4$ for $\rho > 0.43$.

Fig. 7(c) is qualitatively similar to the Fig. 7(b). For example, at $T = 0.125$ the decay exponent η is less than $1/4$ for $\rho > 0.33$. Index η is shown as a function of density ρ for $T = 0.125$ and $T = 0.14$ in Fig. 8. From Fig. 8 one can see that the points corresponding to the condition $\eta = 1/4$ are consistent with the line of isotropic fluid-hexatic phase transition at the phase diagram in Fig. 6(b). The similar results were obtained in Ref. [74] for $\sigma_1 = 1.35$. In principle, this approach can be applied for the construction of the phase diagram, however, it is rather time consuming and cannot give the possibility to calculate the line of the solid-hexatic transition.

It should be noted, that the scaling analysis made in accordance with the algorithm in Refs. [53, 61] also supports the melting scenarios described above. For OOP we used a systems of 102400 particles which were divided in subboxes. The subbox size parameter M is equal to the number of subboxes along the edge of the total system and varies in our simulations from 1 to 16. As expected (see [53, 61]), the bond-orientational order parameter does not change in the ordered region while it

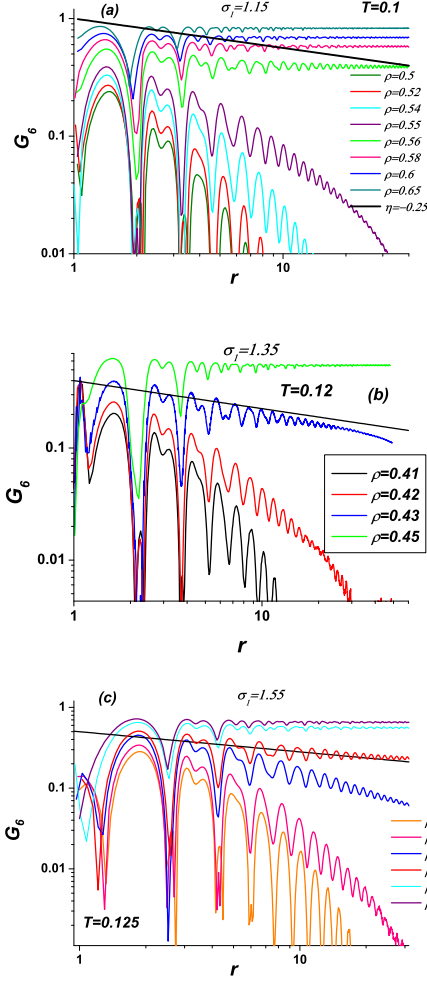


FIG. 7: (Color online) (a) Log-log plots of the orientational correlation function $G_6(r)$ at selected densities across the transition region for $\sigma_1 = 1.15$ and $T = 0.1$. It is seen that the behavior of $G_6(r)$ abruptly changes from isotropic liquid like to the solid-like in accordance with the first-order transition scenario. (b) Log-log plots of the orientational correlation function $G_6(r)$ at selected densities across the hexatic region for $\sigma_1 = 1.35$ and $T = 0.12$. Upon increasing ρ from 0.41 to 0.45 there is a qualitative change in the large-distance behavior of $G_6(r)$, from constant (solid) to power-law decay (hexatic fluid), up to exponential decay (normal fluid). Note that, consistently with the KTHNY theory, the decay exponent η is less than $1/4$ for $\rho > 0.43$; (c) The same as (b) for $\sigma_1 = 1.55$. The decay exponent η is less than $1/4$ for $\rho > 0.33$. Straight lines correspond to the KTHNY prediction $G_6(r) \propto r^{-1/4}$.

increases with increasing the number of the subboxes in the liquid phase. An example of such behavior is shown in Fig. 9 for $\sigma_1 = 1.55$ and $T = 0.1$ and $T = 0.16$.

In the case of $\sigma_1 = 1.35$ the similar analysis was made for the melting of the square lattice region of the phase diagram, and it was shown that the square lattice melts through the first-order phase transition.

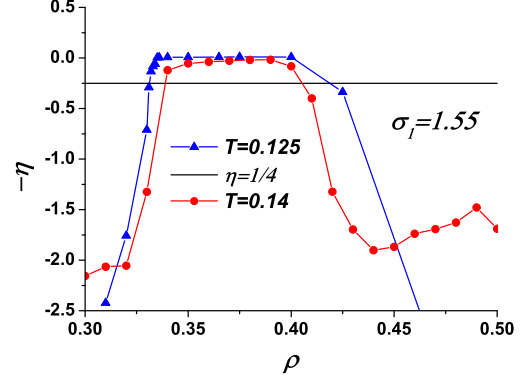


FIG. 8: (Color online) Index η as a function of density for $\sigma_1 = 1.55$ and $T = 0.125$ and $T = 0.14$. Horizontal line corresponds to $\eta = 1/4$.

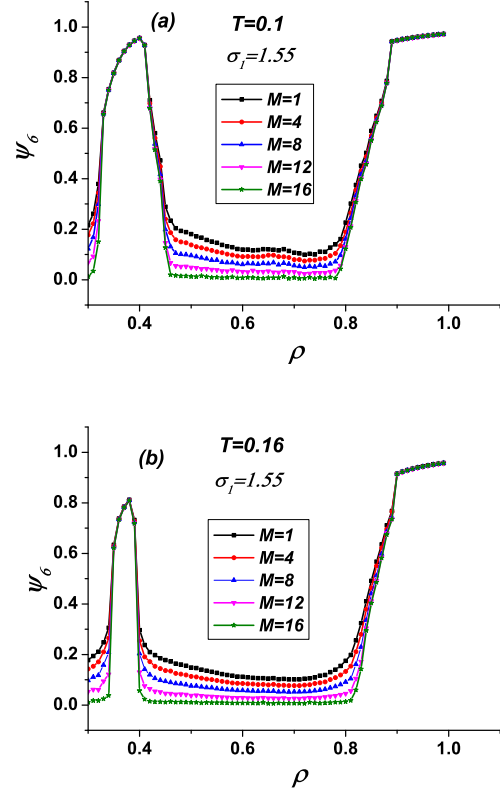


FIG. 9: (Color online) Bond orientational order parameter ψ_6 for $\sigma_1 = 1.55$ and $T = 0.1$ (a) and $T = 0.16$ (b) as a function of density ρ for selected subbox sizes $L = S/M$, for an $S \times S$ system with periodic boundary conditions containing $N = 102400$ particles. Note that the shape of the simulation box is a parallelepiped compatible with the triangular lattice structure, and the parameter M is equal to the number of subboxes along the edge of the total system.

CONCLUSIONS

In conclusion, we have compared the phase diagrams of two-dimensional (2D) classical particles repelling each other through an isotropic core-softened potential for three values of the soft core $\sigma_1 = 1.15; 1.35; 1.55$ corresponding to the increasing softness of the potential from the almost vanishing to rather large. For the smallest value of the soft core, the potential of the system (1) is close to the ordinary soft sphere potential $U(r) \propto r^{-\frac{1}{14}}$. It is widely believed that the 2D systems with hard potentials melt through the weak first-order transition. We found that the system with $\sigma_1 = 1.15$ follows this melting scenario in all range of the thermodynamic parameters. On the other hand, one expects that the 2D melting scenario is in accordance with the KTHNY one for the softer potentials. For larger values of the soft core $\sigma_1 = 1.35; 1.55$, the behavior of the system described by the potential (1) is determined by the soft long-range part of the potential at low densities. The hard core of the potential plays the main role at the high densities and temperatures. It seems that this is the reason of the observed peculiarities of the phase diagrams (see Fig. 6). We have provided the evidences of the occurrence of two-stage continuous reentrant melting via a hexatic phase in the 2D core-softened model at low densities and validated a number of KTHNY predictions for this part of the phase diagram. At the same time, at high densities the melting occurs through the conventional first-order phase transition.

These results may be useful for the qualitative understanding the behavior of the systems with thermodynamic and dynamic anomalies including the water monolayers confined between two hydrophobic plates [21–24, 26, 27].

ACKNOWLEDGMENTS

We are grateful to S. M. Stishov, V. V. Brazhkin, and O.B. Tsiok for stimulating discussions and M.V. Kondrin for the help in computer simulations. Yu.F. and E.T. also thank the Russian Scientific Center Kurchatov Institute and Joint Supercomputing Center of the Russian Academy of Science for computational facilities. The work was supported by the Russian Scientific Foundation (Grant No 14-12-00820).

-
- [1] H. E. Stanley, S. V. Buldyrev, G. Franzese, P. Kumar, F. Mallamace, M. G. Mazza, K. Stokely, and L. Xu, *J. Phys.: Condens. Matter* **22**, 284101 (2010).
 - [2] U. Raviv, P. Laurat, and J. Klein, *Nature* **413**, 51 (2001).
 - [3] P. Gallo, M. Rovere, and S.-H. Chen, *J. Phys. Chem. Lett.* **1**, 729 (2010).

- [4] M. Rovere and P. Gallo, *Eur. Phys. J. E* **12**, 77 (2003).
- [5] Y.D. Fomin, N.V. Gribova, V.N. Ryzhov, S.M. Stishov, and D. Frenkel, *J. Chem. Phys.* **129**, 064512 (2008).
- [6] N.V. Gribova, Y.D. Fomin, D. Frenkel, and V.N. Ryzhov, *Phys. Rev. E* **79**, 051202 (2009).
- [7] Y.D. Fomin, E.N. Tsiok, and V.N. Ryzhov, *J. Chem. Phys.* **135**, 234502 (2011).
- [8] Y.D. Fomin, E.N. Tsiok, and V.N. Ryzhov, *European Physical Journal - Special Topics* **216**, 165 (2013).
- [9] R.E. Ryltsev, N.M. Chtchelkatchev, and V.N. Ryzhov, *Phys. Rev. Lett.* **110**, 025701 (2013).
- [10] Y.D. Fomin, E.N. Tsiok, and V.N. Ryzhov, *Phys. Rev. E* **87**, 042122 (2013).
- [11] S.V. Buldyrev, G. Malescio, C.A. Angell, N. Giovambattista, S. Prestipino, F. Saija, H.E. Stanley, and L. Xu, *J. Phys.: Condens. Matter* **21**, 504106 (2009).
- [12] P. Vilaseca and G. Franzese, *Journal of Non-Crystalline Solids* **357**, 419 (2011).
- [13] G. Franzese, *J. Mol. Liq.* **136**, 267 (2007).
- [14] P. Vilaseca and G. Franzese, *J. Chem. Phys.* **133**, 084507 (2010).
- [15] J. A. Abraham, S. V. Buldyrev, and N. Giovambattista, *J. Phys. Chem. B* **115**, 14229 (2011).
- [16] A. B. de Oliveira, P. A. Netz, T. Colla, and M. C. Barbosa, *J. Chem. Phys.* **125**, 124503 (2006).
- [17] A. B. de Oliveira, P. A. Netz, and M. C. Barbosa, *Europhys. Lett.* **85**, 36001 (2009).
- [18] S. Prestipino, F. Saija, and P.V. Giaquinta, *J. Chem. Phys.* **137**, 104503 (2012).
- [19] S. Prestipino, F. Saija, and G. Malescio, *J. Chem. Phys.* **133**, 144504 (2010).
- [20] M.R. Sadr-Lahijany, A. Scala, S.V. Buldyrev, H.E. Stanley, *Phys. Rev. Lett.* **81**, 4895 (1998).
- [21] L.B. Krott and M.C. Barbosa, *J. Chem. Phys.*, **138** 084505 (2013).
- [22] A.M. Almudallal, S.V. Buldyrev, and I. Saika-Voivod, *J. Chem. Phys.*, **137** 034507 (2012).
- [23] L.B. Krott and J.R. Bordinb, *J. Chem. Phys.* **139**, 154502 (2013).
- [24] L. B. Krott and M. C. Barbosa, *Phys. Rev. E* **89**, 012110 (2014).
- [25] P.A. Netz, F.V. Starr, H.E. Stanley, and M.C. Barbosa, *J. Chem. Phys.* **115**, 344 (2001).
- [26] M. Alcoutlabi and G. B. McKenna, *J. Phys.: Condens. Matter* **17**, R461 (2005).
- [27] S.A. Rice, *Chem. Phys. Lett.* **479**, 1 (2009).
- [28] N. D. Mermin, *Phys. Rev.* **176**, 250 (1968).
- [29] B.I. Halperin and D.R.Nelson, *Phys. Rev. Lett.* **41** 121 (1978).
- [30] D.R.Nelson and B.I. Halperin, *Phys. Rev. B* **19** 2457 (1979).
- [31] A.P. Young, *Phys. Rev. B* **19** 1855 (1979).
- [32] M. Kosterlitz and D.J. Thouless, *J. Phys. C* **6** 1181 (1973).
- [33] C.C. Grimes and G. Adams, *Phys. Rev. Lett.* **42**, 795 (1979).
- [34] Urs Gasser, C. Eisenmann, G. Maret, and P. Keim, *ChemPhysChem* **11**, 963 (2010).
- [35] K. Zahn and G. Maret, *Phys. Rev. Lett.* **85** 3656 (2000).
- [36] P. Keim, G. Maret, and H.H. von Grunberg, *Phys. Rev. E* **75**, 031402 (2007).
- [37] S. Deutschlander, T. Horn, H. Lowen, G. Maret, and P. Keim, *Phys. Rev. Lett.* **111**, 098301 (2013).
- [38] T. Horn, S. Deutschlander, H. Lowen, G. Maret, and P.

- Keim, Phys. Rev. E **88**, 062305 (2013).
- [39] K.J. Strandburg, Rev. Mod. Phys. **60**, 161 (1988).
- [40] C. A. Murray and D. H. V. Winkle, Phys. Rev. Lett. **58**, 1200 (1987).
- [41] Y. Tang, A. J. Armstrong, R. C. Mockler, and W. J. O. Sullivan, Phys. Rev. Lett. **62**, 2401 (1989).
- [42] C. A. Murray, W. O. Sprenger, and R. A. Wenk, Phys. Rev. B **42**, 688 (1990).
- [43] C. A. Murray, W. O. Sprenger, and R. A. Wenk, J. Phys.: Condens. Matter **2**, SA385 (1990).
- [44] S.T. Chui, Phys. Rev. B **28**, 178 (1983).
- [45] W. Janke and H. Kleinert, Phys. Rev. B **41**, 6848 (1990).
- [46] V.N. Ryzhov and E.E. Tareyeva, Phys. Rev. B **51** 8789 (1995).
- [47] V.N. Ryzhov and E.E. Tareeva, Zh. Eksp. Teor. Fiz. **108**, 2044 (1995) [J. Exp. Theor. Phys. **81**, 1115 (1995)].
- [48] V.N. Ryzhov and E.E. Tareyeva, Physica A **314**, 396 (2002).
- [49] V.N. Ryzhov and E.E. Tareyeva, Theor. Math. Phys. **130**, 101 (2002)(DOI: 10.1023/A:1013884616321).
- [50] V.N. Ryzhov, Theor. Math. Phys. **88**, 990 (1991) (DOI: 10.1007/BF01027701).
- [51] V.N. Ryzhov, Zh. Eksp. Teor. Fiz. **100**, 1627 (1991) [Sov. Phys. JETP **73**, 899 (1991)].
- [52] J. Lee and K.J. Strandburg, Phys. Rev. B **46**, 11190 (1992).
- [53] H. Weber, D. Marx, and K. Binder, Phys. Rev. B **51**, 14636 (1995).
- [54] C.H. Mak, Phys. Rev. E **73**, 065104 (2006).
- [55] A. Jaster, Europhys. Lett., **42**, 277 (1998).
- [56] A. Jaster, Phys. Lett. A **330**, 120 (2004).
- [57] K. Bagchi, H.C. Andersen, and W. Swope, Phys. Rev. Lett. **76**, 255 (1996).
- [58] K. Bagchi, H.C. Andersen, and W. Swope, Phys. Rev. E **53**, 3794 (1996).
- [59] E.P. Bernard and W. Krauth, Phys. Rev. Lett. **107**, 155704 (2011).
- [60] M. Engel, J.A. Anderson, S.C. Glotzer, M. Isobe, E.P. Bernard, and W. Krauth, Phys. Rev. E **87**, 042134 (2013).
- [61] K. Binder, S. Sengupta, and P. Nielaba, J. Phys.: Condens. Matter **14**, 2323 (2002).
- [62] R. K. Kalia and P. Vashishta, J. Phys. C: Solid State Phys., **14**, L643 (1981).
- [63] J. Q. Broughton, G. H. Gilmer, and J. D. Weeks, Phys. Rev. B **25**, 4651 (1982).
- [64] R. S. Singh, M. Santra, and B. Bagchi, J. Chem. Phys. **138**, 184507 (2013).
- [65] Keola Wierschem and Efstratios Manousakis, Phys. Rev. B **83**, 214108 (2011).
- [66] N. Gribova, A. Arnold, T. Schilling, and C. Holm, J. Chem. Phys. **135**, 054514 (2011).
- [67] P. Bladon and D. Frenkel, Phys. Rev. Lett. **74**, 2519 (1995).
- [68] S.I. Lee and S.J. Lee, Phys. Rev. E **78**, 041504 (2008).
- [69] S. Prestipino, F. Saija, and P.V. Giaquinta, Phys. Rev. Lett. **106**, 235701 (2011).
- [70] R. Zangi and S. A. Rice, Phys. Rev. E **58**, 7529 (1998).
- [71] D. Frydel and S. A. Rice, Phys. Rev. E **68** 061405 (2003).
- [72] D.E. Dudalov, Yu.D. Fomin, E.N. Tsiok, and V.N. Ryzhov, J. Phys.: Conference Series **510**, 012016 (2014) (doi:10.1088/1742-6596/510/1/012016).
- [73] D.E. Dudalov, Yu.D. Fomin, E.N. Tsiok, and V.N. Ryzhov, Phys. Rev. Lett. **112**, 157803 (2014).
- [74] D.E. Dudalov, Yu.D. Fomin, E.N. Tsiok, and V.N. Ryzhov, Soft Matter **10**, 4966 (2014).
- [75] F. H. Stillinger, J. Chem. Phys. **65**, 3968 (1976).
- [76] S. Prestipino, F. Saija, and P. V. Giaquinta, Phys. Rev. E **71**, 050102(R) (2005).
- [77] P. Mausbach and H.-O. May, Fluid Phase Equilib. **249**, 17 (2006).
- [78] P. Mausbach and H.-O. May, Proc. Appl. Math. Mech. **5**, 685 (2005).
- [79] Yu. D. Fomin, V. N. Ryzhov, and N. V. Gribova, Phys. Rev. E **81**, 061201 (2010).
- [80] T. Yoshida and S. Kamakura, Prog. Theor. Phys. **52**, 822 (1974).
- [81] C. Alba-Simionesco, B. Coasne, G. Dosseh, G. Dudziak, K. E. Gubbins, R. Radhakrishnan, and M. Sliwinski-Bartkowiak, J. Phys.: Condens. Matter **18**, R15 (2006).
- [82] Daan Frenkel and Berend Smit, *Understanding molecular simulation (From Algorithms to Applications)*, 2nd Edition (Academic Press, 2002).
- [83] <http://lammmps.sandia.gov/>
- [84] S. Prestipino, F. Saija, G. Malescio, Soft Matter **5**, 2795 (2009).